Clin Neuroradiol (2016) 26:31–37
DOI 10.1007/s00062-014-0324-4

ORIGINAL ARTICLE

Novel Metal Artifact Reduction Techniques with Use of Slice-Encoding Metal Artifact Correction and View-Angle Tilting MR Imaging for Improved Visualization of Brain Tissue near Intracranial Aneurysm Clips

B. Friedrich · M. Wostrack · F. Ringel · Y.-M. Ryang · A. Förschler · S. Waldt · C. Zimmer · M. Nittka · C. Preibisch

Received: 9 April 2014 / Accepted: 17 July 2014 / Published online: 1 August 2014

Abstract
Purpose The MR image quality after intracranial aneurysm clipping is often impaired because of artifacts induced by metal implants. The purpose of the present study was to evaluate the benefit of a new WARP sequence with slice-encoding metal artifact correction (SEMAC) and view-angle tilting (VAT) MR imaging as novel artifact reduction techniques.
Materials and Methods A new WARP TSE (a work-in-progress software package provided by Siemens Healthcare) sequence was implemented for cranial applications based on a turbo spin echo (TSE) sequence. T1- and T2-weighted images with standard and WARP TSE sequences were acquired from 6 patients with 11 clipping sites, and the images were compared based on artifact size and general image quality.
Results T2- and T1-weighted WARP TSE sequences resulted in a highly significant reduction of metal artifacts compared with standard sequences (T2w- WARP TSE: 89.8±1.4%; T1w- WARP TSE: 84.9±2.9%; $p<0.001$) without a substantial loss of image quality.
Conclusion The use of a new WARP TSE sequence after aneurysm clipping is highly beneficial for increasing the diagnostic MR image quality due to a striking reduction of metal artifacts.

Keywords SEMAC · Clip · Artifact · MRI · WARP

B. Friedrich (✉)
Department of diagnostic and interventional Radiology,
University Hospital Leipzig,
Leipzig, Germany
e-mail: benjamin.friedrich@tum.de

B. Friedrich · A. Förschler · C. Zimmer · C. Preibisch
Department of Neuroradiology, Klinikum rechts der Isar,
Ismaningerstr. 22,
81675 Munich, Germany

M. Wostrack · F. Ringel · Y.-M. Ryang
Department of Neurosurgery, Klinikum rechts der Isar,
Munich, Germany

S. Waldt
Department of Radiology, Klinikum rechts der Isar,
Munich, Germany

M. Nittka
Siemens Healthcare,
Erlangen, Germany

Introduction

Patients who are being treated for intracranial aneurysms often need further examination through cranial magnetic resonance imaging (MRI) for a variety of reasons, including postoperative complications (e.g., infection) and the occurrence of other intracranial pathologies (e.g., inflammation or malignancy). Intracranial aneurysms can be treated using either an endovascular approach that involves coiling of the aneurysm with platinum coils or a surgical approach that involves clipping of the aneurysm sack with titanium clips [1]. The implanted endovascular coils only produce a mild artifact on MRI, so the surrounding brain tissue and even the adjacent vessels can be sufficiently distinguished [2]. However, titanium aneurysm clips produce severe artifacts on MRI [3, 4]. Because of the substantial susceptibility difference between brain tissue and titanium, these metallic implants induce large distortions of the local magnetic field [5]. Minor effects also result from gradient- or radio frequency (RF)-induced eddy currents [6, 7]. In addition to intravoxel signal dephasing (and, thus, an extremely shortened T2*), which primarily leads to signal loss in gradient

echo imaging, magnetic susceptibility gradients cause deficient spatial encoding and thereby result in severe signal voids and pile-ups in spin echo images [8].

The artifacts described make it nearly impossible to diagnose alterations in a large area surrounding the aneurysm clip, not to mention the adjacent vessels. All radiologists, neurosurgeons, and neurologists working with intracranial aneurysm patients on a regular basis are aware of this limitation and the difficulties in interpreting MRI images affected by clip artifacts [9].

Generally, imaging with a high spatial resolution and high readout bandwidth, i.e., strong imaging gradients, are known to mitigate the influence of susceptibility gradients. In addition, combined with a small slice thickness, a high RF bandwidth is known to be beneficial for reducing geometric distortions of the slice profile. More elaborate techniques, such as view angle tilting (VAT) [10, 11] and slice-encoding for metal artifact correction (SEMAC) [8, 12], have been developed in recent years. Using VAT, geometric in-plane distortions can be reduced through an additional gradient along the slice selection axis during the readout. This results in a shearing effect in the imaged slice that is equivalent to a tilted view angle [10]. SEMAC combines VAT with a through-plane distortion correction by applying additional phase encoding in the slice selection direction. For a sufficiently high number of encoding steps, a dislocated signal can be recovered [8]. While these new techniques were successfully applied in orthopedic radiological contexts [13, 14] and in the visualization of dental implants [15], they have never before been used in a neuroradiological setting.

The aim of the present study was to apply the dedicated prototype WARP TSE sequence implementing the VAT [10, 11] and SEMAC [8, 12] techniques, to cranial applications in order to provide an improved visualization of surgically implanted aneurysm clips. In addition, the study aimed to compare the acquired images with standard sequences with respect to metal artifacts, general image quality and consequent diagnostic value.

Materials and Methods

A total of 6 patients with 11 clipping sites volunteered and were included in the present study (Table 1). All implanted titanium clips were labeled as MRI safe by the manufacturer (Sugita Aneurysm Clips, Mizuho Medical Inc, Japan). This study was approved by the local ethics committee and followed the Helsinki Guidelines. Written consent was obtained from the volunteers.

A homogeneous gel phantom was used for sequence optimization and signal to noise ratio (SNR) measurements. It consisted of 1.75% agar dissolved in a 0.9% sodium chloride solution and was doped with 0.11 mmol/L of gadolinium diethylenetriamine pentaacetic acid (Gd-DTPA) in order to achieve physiological relaxation times of T1 ≈ 1000 ms and T2 ≈ 65 ms.

Table 1 Patient data

Patient No.	Sex	Age	Site of aneurysm	Surgery → imaging (days)
1	F	56	Left MCA, left ICA	2111
2	F	37	Left MCA, right MCA	45
3	F	74	Right MCA	977
4	M	68	Left MCA, left Pcom	2
5	F	54	Right MCA, right Carotid-T	580
6	M	72	Left ICA, left Pcom	2135

MCA middle cerebral artery, *ICA* internal carotid artery, *Pcom* posterior communicating arteries

MR Imaging

Imaging was performed on a 3 T whole-body MRI scanner (MAGNETOM Verio, Siemens Healthcare, Erlangen, Germany). The MRI protocol comprised standard T1w TSE (TE/TR 11/500 ms) and T2w TSE (TE/TR 87/8700 ms) sequences with a voxel size of $1 \times 1 \times 3$ mm^3. Furthermore, a prototype sequence called WARP TSE (a work-in-progress software package provided by Siemens Healthcare) was applied with T1w (TE/TR 8/500 ms) and T2w (TE/TR 88/8700 ms) contrast and a voxel size of $1 \times 1 \times 1.5$ mm^3. For reduction of metal artifacts, the WARP TSE sequence implements the SEMAC technique [8], including VAT [10, 11] and both a high readout bandwidth and a high RF pulse bandwidth. VAT uses an additional gradient in slice select direction during readout in order to reduce in-plane distortions due to susceptibility gradients [10]. This corresponds to an effective tilt of the acquired slice and may cause image blurring which can be mitigated by high bandwidth readouts [11]. SEMAC addresses through plane distortions by means of additional phase encoding gradients in slice-select direction [8]. The additional phase encoding resolves the extent of the signal excited outside the intended image plane and shifts the signal back to its correct position during image post processing. The WARP TSE sequence, as implemented in the current study, was applied to patients with total hip arthroplasty previously by Sutter et al. [14]. We therefore refer to this study for further implementation details. In preliminary phantom experiments, 10 SEMAC encoding steps, i.e., 10 different additional gradients in slice-select direction, and a readout bandwidth of 501 Hz/Px yielded a reasonable compromise between artifact reduction, measurement time, and SNR for the intended cranial application. The excitation bandwidth of the RF pulse was set to 1.3 kHz because higher values would exacerbate problems with RF-exposure (specific absorption rate—SAR). To maintain the measurement time and SAR within a tolerable range, par-

Table 2 Parameters of imaging sequences

Parameter	Standard TSE T1w	WARP TSE T1w	Standard TSE T2w	WARP TSE T2w
No. slices	30	20	30	30
Slice thickness (mm)	3	1.5	3	1.5
Distance (%)	10	0	10	0
FOV (mm)	256	256	256	256
Matrix	256	256	256	256
Voxel size (mm^3)	1 × 1 × 3	1 × 1 × 1.5	1 × 1 × 3	1 × 1 × 1.5
Trajectory	Cartesian	Cartesian	BLADE	Cartesian
GRAPPA	No	3	2	3
Phase resolution (%)	100	100	89.3	100
Phase partial Fourier	Off	On	n.a.	On
Phase-OS (%)	15	0	50	0
Averages	3	3	1	1
Flip angle	150°	130°	165°	130°
Turbo factor	3	6	15	19
TE (ms)	11	8	87	88
TR (ms)	500	500	8700	8700
BW (Hz/Px)	300	501	160	501
VAT	No	On	No	On
SEMAC steps	n.a.	10	n.a.	10
Acq. duration (min)	2:32	9:03	3:48	7:25

FOV field of view, *GRAPPA* generalized autocalibrating partially parallel acquisitions, *TSE* turbo spin echo, *TE* echo time, *TR* repetition time, *BW* bandwidth, *VAT* view-angle tilting, *SEMAC* slice-encoding metal artifact correction, *Phase-OS* Phase-Oversampling

allel imaging (generalized autocalibrating partially parallel acquisitions—GRAPPA, factor 3), phase partial Fourier, increased turbo factors, and reduced refocusing flip angles were used. Detailed imaging parameters of standard and WARP sequences are listed in Table 2.

The volumes of the clip artifacts in the standard and the WARP sequences were manually assessed. This was accomplished by manual measurement of the artifact area inhibiting a clear anatomical distinction on every slice and multiplying the area by the slice thickness. Afterwards, the differences in the artifact volume between standard and WARP sequences were calculated. This process was independently performed by two experienced neuroradiologists (Benjamin Friedrich, Simone Waldt), and the mean between both raters was used here. In addition, the correlation between both raters was calculated.

The SNR was evaluated in the phantom in accordance with the NEMA method 1 as described by Goerner & Clarke [16]. Each imaging protocol was measured twice with a time delay of approximately 25 min, which was determined by the duration of the imaging protocol. For each method, the average and difference of the two acquired data sets were calculated. The mean signal ⟨S⟩ was determined from the average image as the mean of a large circular region of interest (ROI) in the center of the homogenous phantom region. The noise was determined from the same ROI in the subtraction image as the standard deviation (SD) of the signal differences according to Goerner & Clarke [16]:

$$SD = \left[\frac{\sum_{i=1}^{n} \sum_{j=1}^{m_i} \left(R_{i,j} - \langle R \rangle \right)^2}{\sum_{i=1}^{n} m_i - 1} \right]^{1/2}$$

where ⟨R⟩ is the mean signal difference within the ROI, $R_{i,j}$ are the individual signal differences at pixel numbers i and j within the ROI, and n and m are the pixel numbers in the row and column directions. SNR was then calculated as $SNR = \frac{\langle S \rangle}{SD/\sqrt{2}}$. This measurement was repeated twice for statistical evaluation.

Finally, the general image quality of the standard TSE and the WARP TSE patient scans was rated by two experienced neuroradiologists (Benjamin Friedrich, Simone Waldt) using a five-point Likert scale and ignoring the clip artifact (1: ‘extremely poor’ defined as “the images are not clinically useful”; 2: ‘poor’ defined as “clinical use is not advised”; 3: ‘average’ defined as “borderline clinical use due to the image quality”; 4: ‘good’ defined as “containing no substantial adverse effect for clinical use”; and 5: ‘excellent’ defined as “no restrictions for clinical use”).

Statistical Analysis

Statistical analysis was performed using the software SigmaPlot 11. The artifact volumes were compared using Student’s t-test. The correlation between the two reviewers concerning the artifact volume was calculated using a Pearson correlation. The results of the assessment for image quality were analyzed using a Student’s t-test. For comparison of the SNR measurement a Mann-Whitney Rank Sum test was performed. Statistical significance was assumed at $p < 0.05$. All values given are the mean ± SD.

Results

In the standard T2-weighted and T1-weighted sequences, a large area of brain tissue could not be examined due to the artifacts induced by the implanted aneurysm clips. The WARP TSE sequences on the other hand resulted in an impressive reduction in the metal artifacts. Therefore, the assessment of the surrounding brain tissue was considerably improved (Fig. 1). This impression could also be quantified. While the average clip artifact had a volume of 84 ± 63 cm^3 and 57 ± 52 cm^3 in the T2w and T1w sequences, respectively, with WARP TSE the artifact volume could be reduced to 9 ± 8 cm^3 in T2-weighted images and 10 ± 9 cm^3

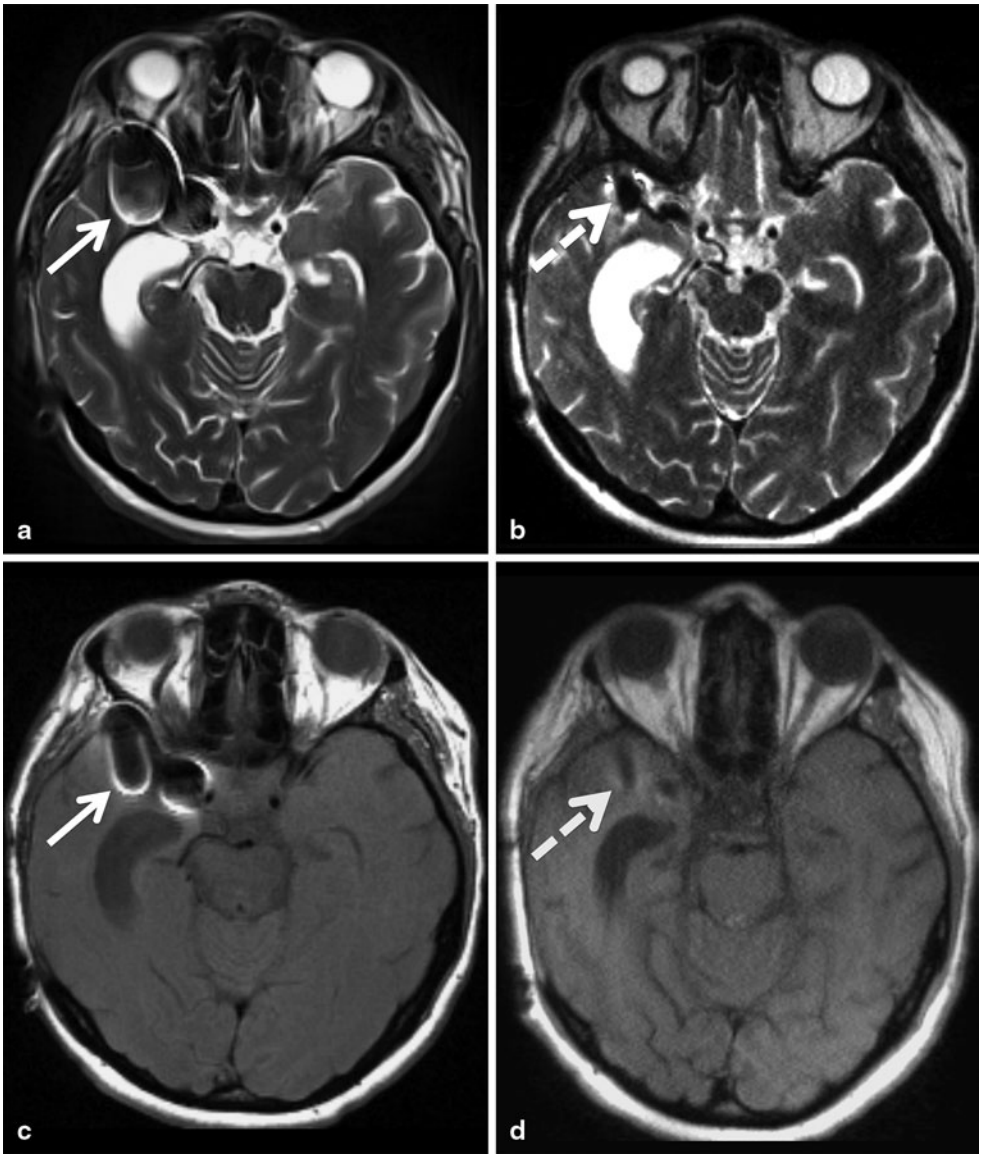

Fig. 1 Comparison of WARP TSE T2w (**b**) and T1w (**d**) sequences with standard TSE T2w (**a**) and T1w (**c**) sequences. In the images acquired with the standard sequences, large metal artifacts (*solid arrow*) after clipping of a right-sided MCA aneurysm diminish the diagnostic quality in both T2w images (**a**) and in T1w images (**c**). With the new WARP TSE sequences a substantial reduction of clip-induced metal artifacts (*dashed arrow*) was achieved (**b**, **d**)

in T1-weighted images ($p<0.001$) (Fig. 2). The artifact could be clearly distinguished from the surrounding brain tissue as both raters showed a highly significant correlation in their independently obtained findings ($R=0.91$) (Fig. 3a).

T1- as well as T2-weighted images showed a substantial drop in SNR when images without and with WARP were compared. Repeated SNR measurements in the homogenous gel phantom revealed 108.9±22.5 and 49.7±12.4 for the T1-weighted scans, and 147.7±23.8 and 44.8±7.3 for the T2-weighted scans without and with WARP, respectively.

The general image quality of the standard TSE sequences was rated very close to 'excellent' in both T1w and T2w images (both 4.66±0.51). The drop in SNR was reflected by a decrease in the general image quality of 14.1% and 7.1% on T1w and T2w images, respectively, using the WARP TSE sequences. Nevertheless, the general images quality remained 'good' in both T1w and T2w WARP TSE sequences (4±0; 4.33±0.51) (Fig. 3b).

The statistical results are summarized in Table 3.

To emphasize the benefit of the WARP sequences in reducing metal artifacts, we present an exemplary case. Almost 10 years ago, a patient was surgically treated for a symptomatic cavernoma in the right basal ganglia and the frontal pole of the temporal lobe (Fig. 4a). Then 5 years later, a benign aneurysm of the right middle cerebral artery was diagnosed and treated by surgical clipping. The follow-up MRI imaging of the former cavernoma site was markedly impaired by the large metal artifacts (Figs. 4b and 4d). With the new WARP sequences presented here, the entire resection area could be clearly assessed and no evidence of a recurrence of the cavernoma could be found (Figs. 4c and 4e).

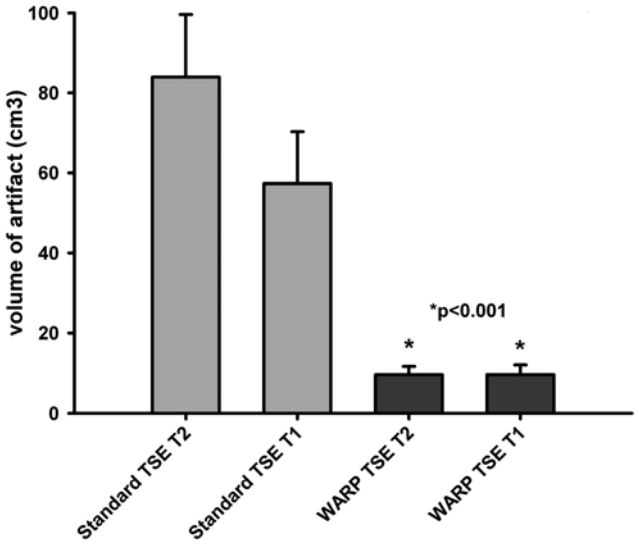

Fig. 2 The application of the new WARP TSE sequences results in a substantial reduction (of approximately 90%) of the artifact volume induced by metal aneurysm clips

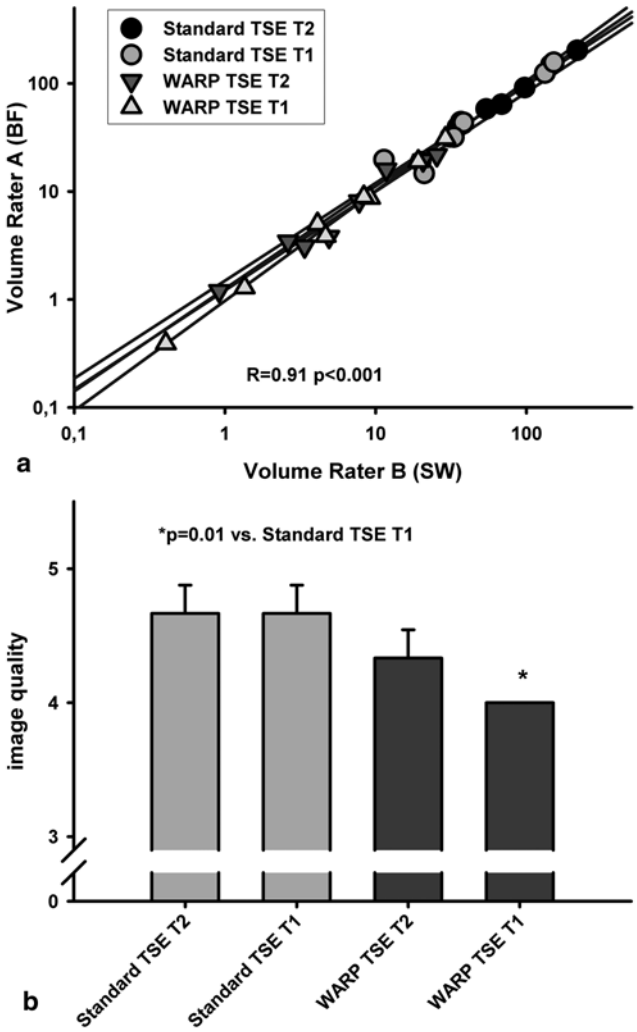

Fig. 3 Both independent raters could clearly distinguish the artifact induced by the aneurysm clip as shown by the highly significant correlation of their measurements (**a**). The general image quality of the standard TSE image sequences was rated almost 'excellent'. Although a decrease in the general image quality occurred when using the WARP TSE sequences, the general image quality remained 'good' (**b**)

Discussion

In this report, we present results from the dedicated prototype WARP TSE sequence, a method that combines SEMAC with high readout and RF pulse bandwidths for metal artifact suppression, in order to improve diagnostic quality after surgical aneurysm treatment.

Large metal artifacts induced by aneurysm clips are a well-known issue impairing the diagnostic quality and value of MRI examinations after clipping. If a specific concern is raised about tissue in the vicinity of the implanted metal clip, an educated guess has to be made or additional imaging performed. Additional imaging typically involves x-ray-dependent methods, such as computed tomography (which is associated with diminished soft-tissue contrast), or angiography (which is associated with the risk of potential harm from the intervention and the large amounts of ionic contrast agent that are used). Therefore, an MRI-based method is urgently needed.

Our results demonstrate a striking reduction of artifacts from susceptibility-related magnetic field gradients originating from the metal implants. However, the application of SEMAC encoding leads to an increase in measurement time because the entire imaging experiment has to be repeated for each encoding step. Tolerable measurement times can be achieved by applying phase partial Fourier and parallel imaging techniques at the expense of SNR. In contrast, VAT is accompanied by image blurring [10, 11], which, at the expense of SNR, can be reduced by a high readout bandwidth and thin slices. Thus, a perfect suppression of metal artifacts either requires prohibitively long measurement times or yields unacceptably low SNR. A compromise has to be found between artifact reduction, sufficient SNR, and tolerable measurement time. At 3 T, matters are exacerbated by the fact that TSE sequences are limited by a high SAR. This is especially critical for the T1w sequence, in which a smaller turbo factor (shorter echo train) and the lower intrinsic SNR reduce the scan efficiency. In addition, the number of slices is limited by SAR.

Currently, one of the major disadvantages of using SEMAC sequences is the long time needed to acquire the images. In our setting, a SEMAC T2-weighted scan has an acquisition time of 7 min, a SEMAC T1-weighted scan takes up to 9 min. As the long scanning time of WARP sequences prohibit repetition of the scan in a second or even third orientation, we reduced the voxel size of the WARP sequences to be able to perform three-dimensional reformatting and

Table 3 Statistical results

	Standard TSE T1w	WARP TSE T1w	Reduction (%)	*p* value	Standard TSE T2w	WARP TSE T2w	Reduction (%)	*p* value
Volume of artifact	57 ± 52 cm^3	10 ± 9 cm^3	85	< 0.001	84 ± 63 cm^3	9 ± 8 cm^3	90	< 0.001
SNR	108.9 ± 22.5	49.7 ± 12.4	54.4	< 0.001	147.7 ± 23.8	44.8 ± 7.3	69.7	< 0.001
Image quality	4.66	4	14.1	0.01	4.66	4.33	7.1	0.21

TSE turbo spin echo, *SNR* signal to noise ratio

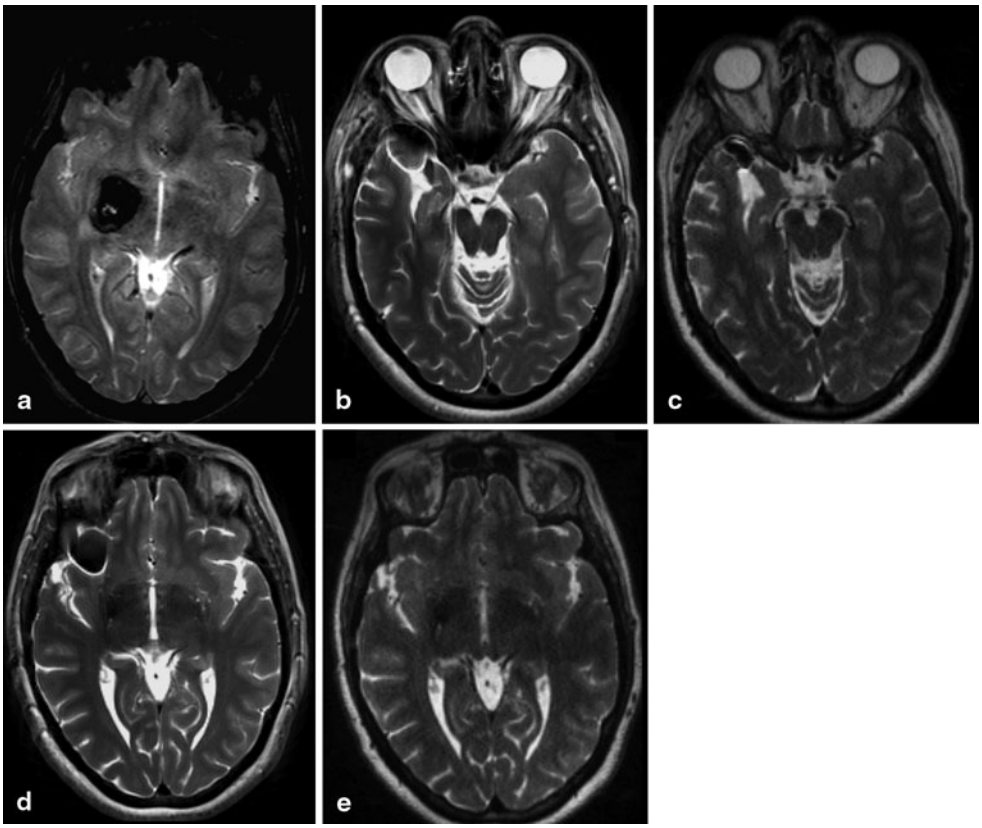

Fig. 4 The case of a patient initially treated for a symptomatic cavernoma (**a**; T2* weighted image). A few years later, the patient was treated for a right-sided MCA aneurysm by surgical clipping. In the follow-up MRI scans, large metal artifacts compromised the site of the former cavernoma (**b**, **d**; T2w TSE). With the WARP TSE sequences it is now possible to evaluate the entire site of the former cavernoma without interference from artifacts (**c**, **e**; T2w WARP TSE)

therefore compensate for the missing scans in different planes. Although this scanning time is quite long, the indication for the MRI is usually a specific question that cannot be answered using a different examination method, and this justifies such a prolonged scanning time. Additionally it can be expected that future developments in both hardware and software will further accelerate the image acquisition process.

In our current study, for T1-weighted images WARP TSE resulted in an approximately 54 % loss of SNR compared with standard T1w TSE sequences. This was inspite of the fact that the additional SEMAC encoding increases the SNR. The reasons for the observed loss of SNR are the 50 % reduction in slice thickness, the use of phase partial Fourier and parallel imaging (GRAPPA, factor 3), while the standard sequence exhibits full sampling of k-space. Similar to the T1w sequences, we measured an SNR loss of 70 % in T2w images. In this case, the standard sequence already applied undersampling (GRAPPA, factor 2) in combination with BLADE sampling, which is less efficient than plain Cartesian sampling. Although both T1-weighted and T2-weighted SEMAC images have enough signal to provide an excellent diagnostic quality, future developments should target an enhancement of SNR.

Besides that, a desirable goal for future developments is further reduction of the artifact to allow visualization of the adjacent vessels in the area treated, for example, to study incompletely occluded aneurysms.

In summary, we implemented a new application of the SEMAC technique in MRI to reduce metal artifacts induced by aneurysm clips. For the first time, this gives the opportunity to investigate pathologies in the area of the clip, e.g., malignant processes, chronic inflammatory processes, infarction, or infection. Furthermore, this opens up a com-

pletely new scientific field to investigate short- and long-term changes and reactions of brain tissue to implanted titanium aneurysm clips.

Acknowledgment We thank Siemens Healthcare for providing a work-in-progress software package (WARP WIP for Orthopedic Implant Imaging).

Conflict of Interest None.

References

1. Molyneux A, Kerr R, Stratton I, Sandercock P, Clarke M, Shrimpton J, Holman R, International Subarachnoid Aneurysm Trial (ISAT) Collaborative Group. International Subarachnoid Aneurysm Trial (ISAT) of neurosurgical clipping versus endovascular coiling in 2143 patients with ruptured intracranial aneurysms: a randomised trial. Lancet. 2002;360:1267–74.
2. Majoie CB, Sprengers ME, van Rooij WJ, Lavini C, Sluzewski M, van Rijn JC, den Heeten GJ. MR angiography at 3T versus digital subtraction angiography in the follow-up of intracranial aneurysms treated with detachable coils. AJNR Am J Neuroradiol. 2005;26:1349–56.
3. Romner B, Olsson M, Ljunggren B, Holtas S, Säveland H, Brandt L, Persson B. Magnetic resonance imaging and aneurysm clips. Magnetic properties and image artifacts. J Neurosurg. 1989;70:426–31.
4. Olsrud J, Lätt J, Brockstedt S, Romner B, Björkman-Burtscher IM. Magnetic resonance imaging artifacts caused by aneurysm clips and shunt valves: dependence on field strength (1.5 and 3 T) and imaging parameters. J Magn Reson Imaging. 2005;22:433–7.
5. Lüdeke KM, Röschmann P, Tischler R. Susceptibility artefacts in NMR imaging. Magn Reson Imaging. 1985;3:329–43.
6. Graf H, Steidle G, Martirosian P, Lauer UA, Schick F. Metal artifacts caused by gradient switching. Magn Reson Med. 2005;54:231–4.
7. Camacho CR, Plewes DB, Henkelman RM. Nonsusceptibility artifacts due to metallic objects in MR imaging. J Magn Reson Imaging. 1995;5:75–88.
8. Lu W, Pauly KB, Gold GE, Pauly JM, Hargreaves BA. SEMAC: Slice Encoding for Metal Artifact Correction in MRI. Magn Reson Med. 2009;62:66–76.
9. Wichmann W, Von Ammon K, Fink U, Weik T, Yasargil GM. Aneurysm clips made of titanium: magnetic characteristics and artifacts in MR. AJNR Am J Neuroradiol. 1997;18:939–44.
10. Cho ZH, Kim DJ, Kim YK. Total inhomogeneity correction including chemical shifts and susceptibility by. Med Phys. 1988;15:7–11.
11. Butts K, Pauly JM, Gold GE. Reduction of blurring in view angle tilting MRI. Magn Reson Med. 2005;53:418–24.
12. Hargreaves BA, Chen W, Lu W, Alley MT, Gold GE, Brau AC, Pauly JM, Pauly KB. Accelerated slice encoding for metal artifact correction. J Magn Reson Imaging. 2010;31:987–96.
13. Chen CA, Chen W, Goodman SB, Hargreaves BA, Koch KM, Lu W, Brau AC, Draper CE, Delp SL, Gold GE. New MR imaging methods for metallic implants in the knee: artifact correction and clinical impact. J Magn Reson Imaging. 2011;33:1121–7.
14. Sutter R, Ulbrich EJ, Jellus V, Nittka M, Pfirrmann CW. Reduction of metal artifacts in patients with total hip arthroplasty with slice-encoding metal artifact correction and view-angle tilting MR imaging. Radiology. 2012;265:204–14.
15. Zho SY, Kim MO, Lee KW, Kim DH. Artifact reduction from metallic dental materials in T1-weighted spin-echo imaging at 3.0 T. J Magn Reson Imaging. 2013;37:471–8.
16. Goerner FL, Clarke GD. Measuring signal-to-noise ratio in partially parallel imaging MRI. Med Phys. 2011;38:5049–57.